LATITUDINAL DEPENDENCE OF RADIATIVELY DRIVEN MASS LOSS FROM RAPIDLY ROTATING HOT-STARS

S. P. OWOCKI

Bartol Research Institute, University of Delaware, Newark, DE 19716

S. R. CRANMER

Harvard-Smithsonian Center for Astrophysics, Cambridge, MA 02138

AND

K. G. GAYLEY

Department of Physics and Astronomy, University of Iowa, Iowa City, IA 50011

Abstract. We investigate the latitudinal variation of radiatively driven mass loss from rapidly rotating hot-stars. Previous analyses have assumed a uniformly bright stellar surface and concluded that the wind mass flux and density should increase with the increased centrifugal force toward the wind *equator*. In contrast, we show here that a gravity darkening in which the surface radiation flux scales with the effective (centrifugally reduced) gravity leads to a dramatically different wind morphology, with the strongest mass loss now occurring toward the relatively bright *poles*. We also review recent work that indicates nonradial (poleward) components of the line-driving force in such rotating winds can effectively inhibit the equatorward wind deflection needed to form an equatorial wind-compressed disk. Finally, we examine the equatorial bistability model, and show that a sufficiently strong jump in wind driving parameters can, in principle, overcome the effect of reduced radiative driving flux, thus still allowing moderate enhancements in density in an equatorial, bistability zone wind.

1. Introduction

Several observational reviews of this workshop (e.g. Zickgraf) have emphasized the various lines of evidence that the circumstellar regions around B[e] stars have an enhanced equatorial density, possibly even a circumstellar disk. A key question is whether this enhanced equatorial density might be a direct result of rotational effects that could influence the latitudinal variation of the radiatively driven stellar wind expected from such a luminous B-star. Previous theoretical analyses of winds from rotating hot stars have examined various effects that can increase the equatorial density, including:

- enhanced mass flux and reduced wind speed associated with the centrifugally reduced effective gravity near the equator (Friend and Abbott 1986; Pauldrach, Puls, and Kudritzki 1986);
- Wind Compressed Disks (WCDs) (Bjorkman & Cassinelli 1993; Owocki, Cranmer, and Blondin 1994; Ignace, Cassinelli, and Bjorkman 1996); or
- enhanced mass loss from a "bi-stability zone" triggered by the reduced radiation temperature near the equator (Lamers and Pauldrach 1991).

All these previous analyses have implicitly assumed that the radiative flux is uniformly distributed over the stellar surface. However, to the extent that radiation dominates the energy transport in the envelopes of such hot stars, the classical analysis of von Zeipel (1924) implies a "gravity-darkening" effect, in which the radiative flux from near the equator is reduced in proportion to the centrifugally reduced effective gravity there. Here we review results from recently developed 2-D wind simulations that incorporate the effects of such gravity darkening, as well as nonradial components of the line-driving force (Owocki, Cranmer, and Gayley 1996). As discussed below, both effects turn out to have a surprisingly strong impact on the latitudinal mass distribution of a stellar wind. To provide a basis for understanding these unexpected results, let us first review scaling relations predicted from 1-D models of line-driven winds.

2. Scaling Laws from 1-D Models

Initial investigations (Friend & Abbott 1986; Pauldrach et al. 1986) of the possible role of rotation on radiatively driven winds derived 1-D models based on the standard line-driving formalism of Castor, Abbott, and Klein (1975; hereafter CAK), but now adding the effect of an outward centrifugal acceleration in the equatorial plane, $g_{cent}(r) = V_{rot}^2 R^2/r^3$, where V_{rot} is the equatorial rotation speed at the stellar surface radius $r = R$. Although this centrifugal term declines faster with radius than gravity, the mass loss is fixed at a critical point quite near the stellar surface. This suggests that

the effect on the local mass flux at any colatitude θ of a rotating star can be written in terms of a centrifugally reduced, *effective* surface gravity

$$g_{eff}(\theta) = \frac{GM}{R^2}\left(1 - \Omega \sin^2\theta\right), \tag{1}$$

where G and M are the gravitation constant and stellar mass, and $\Omega \equiv V_{rot}^2 R/GM$. We thus rewrite the standard CAK mass loss rate scaling law (i.e. CAK eqn. (46)) in terms of *surface* values of the mass flux $\dot{m} = \rho v$, radiative flux F, and effective gravity g_{eff}, relative to corresponding polar ($\theta = 0$) values $\dot{m}_o$, F_o, and $g_o = GM/R^2$,

$$\frac{\dot{m}(\theta)}{\dot{m}_o} = \left[\frac{F(\theta)}{F_o}\right]^{1/\alpha} \left[\frac{g_{eff}(\theta)}{g_o}\right]^{1-1/\alpha}, \tag{2}$$

where α is the usual CAK exponent, assumed here to be constant at all latitudes (cf. §4.2 below).

For example, if we take $F(\theta) = F_o$, then we obtain the scaling

$$\frac{\dot{m}(\theta)}{\dot{m}_o} = \left[1 - \Omega \sin^2\theta\right]^{1-1/\alpha} \quad ; \quad F(\theta) = F_o\,, \tag{3}$$

which, for $\sin\theta = 1$ and $\alpha \approx 0.6$, provides a reasonably good fit to, e.g., numerical results plotted in fig. 4 of Friend & Abbott 1986. Since $\alpha < 1$, the exponent $1 - 1/\alpha$ is negative, implying that the mass flux increases monotonically from pole ($\sin\theta \to 0$) toward the equator ($\sin\theta \to 1$). On the other hand, if we apply the standard von Zeipel(1924) (see also Kippenhahn & Weigert 1990) gravity darkening law that the surface flux itself varies in proportion to the centrifugally reduced effective gravity, $F(\theta) \sim g_{eff}$, we obtain

$$\frac{\dot{m}(\theta)}{\dot{m}_o} = 1 - \Omega \sin^2\theta \quad ; \quad F(\theta) \sim g_{eff}(\theta) \tag{4}$$

so that the mass flux now *decreases* towards the equator, with a maximum at the *pole* (see §4)!

Friend and Abbott (1986) likewise find that the terminal wind speed is decreased by rotation in the equator. We can also approximate this result within our 1-D concept of a centrifugally reduced gravity to predict a latitudinally varying wind terminal speed that scales with an effective escape speed, $v_\infty(\theta) \sim v_{esc}\sqrt{1 - \Omega \sin^2\theta}$. The latitudinal variation of density is then obtained from $\rho \sim \dot{m}/v_\infty$.

3. 2-D Dynamical Simulations of Rotating Winds

3.1. EQUATORIAL WIND COMPRESSED DISKS

A major advance in modelling rotating hot-star winds was development of the elegantly simple "Wind Compressed Disk" (WCD) paradigm by Bjork-

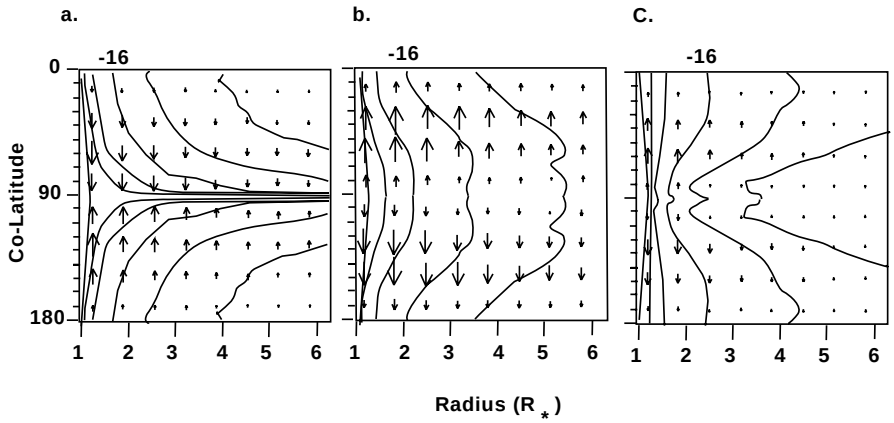

Figure 1. Contours of stellar wind density plotted vs. colatitude θ and radius r, spaced logarithmically with two contours per decade, with label denoting the contour for $\rho = 10^{-16}$g/cm^3. The superposed vectors represent the latitudinal velocity, with the maximum length corresponding to a magnitude of $v_\theta = 100$ km/s. The three panels show the cases (a) without nonradial forces or gravity darkening, (b) with nonradial forces but no gravity darkening, and (c) with both nonradial forces and gravity darkening.

man & Cassinelli (1993). They noted that, like satellites launched into earth orbit, parcels of gas gradually driven radially outward from a rapidly rotating star should remain in a tilted 'orbital plane' that brings them over the equator. As wind parcels from opposite hemispheres collide over the equator, they form a disk of compressed gas. A key simplification here is to assume that, like gravity, the radiative driving is a radially directed, *central* force, so that the total angular momentum of each individual wind fluid parcel is conserved, fixed by the rotation at its initial latitude at the wind base (i.e., at the subsonic stellar surface), and remaining in a fixed plane perpendicular to the angular momentum vector. The crucial criterion for the formation of a disk is that the near-star wind speed not be too much larger than the rotation speed. For lower rotation or faster winds, material may not be deflected into a disk, but still can form a more modest equatorial density enhancement, a "Wind Compressed Zone" (WCZ; Ignace, Cassinelli, and Bjorkman 1996).

To test this WCD paradigm, Owocki, Cranmer, and Blondin (1994) carried out 2-D hydrodynamical simulations of line-driven winds from rotating hot-stars. In keeping with the original WCD model, they assumed a purely radial driving force, though now computed dynamically using the finite-disk, spherical-star form of the usual CAK line-driving formalism (Friend

& Abbott 1986; Pauldrach et al. 1986). The results, shown in figure 1a for their standard 'S-350' model (a B2 star with $V_{rot} = 350$ km/s), generally confirm the basic tenets of the WCD model, with certain detailed modifications (e.g., infall of inner disk material). The overall wind morphology consists of a relatively fast, low-density polar wind, plus a dense equatorial disk with slow outflow in its outer part. Figure 1a shows density contours for this standard WCD case, plotted vs. radius and colatitude, with superposed vectors representing the magnitude and sense of the latitudinal velocity component $v_\theta(r,\theta)$. The WCD, manifest here by the strong equatorial extension of higher density contours, is the direct result of the flow compression associated with the equatorward sense of the latitudinal velocity from both the northern and southern hemispheres.

3.2. INHIBITION OF WCD BY POLEWARD LINE-FORCE COMPONENT

For rotating stars, the line acceleration can generally also have *nonradial* components. Within the CAK formalism of a fixed ensemble of lines with a power-law number distribution in opacity, its vector form is given by integration over solid angle Ω_* of the stellar core intensity I (Cranmer and Owocki 1995),

$$\mathbf{g}^{\rm rad}(\mathbf{r}) = \frac{K}{W^\delta \rho(\mathbf{r})^{\alpha-\delta} c} \int_\Omega d\Omega\, \mathbf{n}\, I(\mathbf{n},\mathbf{r})\, \{\mathbf{n}\cdot\nabla\,[\mathbf{n}\cdot\mathbf{v}(\mathbf{r})]\}^\alpha \ , \qquad (5)$$

where K is proportional to the usual CAK line-normalization constant k, and the exponent δ accounts for the ionization-state dependence on density ρ and dilution factor W (Abbott 1982). Note that the weighting for the force contribution of each ray along a direction $\mathbf{n}$ is proportional to the projected velocity gradient in that direction, $\mathbf{n}\cdot\nabla\,[\mathbf{n}\cdot\mathbf{v}(\mathbf{r})]$.

Owocki, Cranmer, and Gayley (1996) carried out simulations of rotating winds including these nonradial line-force components. Figure 1b shows the corresponding wind density structure for the S-350 model, still assuming a uniformly bright stellar core. As predicted in the above 1-D analysis, the reduced gravity, enhanced mass loss, and lower flow speed near the equator yield a broad, moderate density enhancement in the equatorial wind. But there is *no wind compressed disk*! Indeed, the sense of the superposed vectors is now reversed, indicating that the latitudinal velocity is now *away from the equator*. As such, there is no longer any wind compression effect, and so the tendency to form a WCD is completely inhibited.

This latitudinal flow reversal is a direct consequence of a *poleward* component of the line-force, which arises primarily from asymmetries in the line-of-sight velocity gradient, operating through the velocity-gradient weighting of the angle integral in eqn. (5). The lower effective gravity near the equator

implies generally lower outflow speeds there, and thus from most midlatitude locations in the wind, the line-of-sight velocity gradient is stronger when looking toward the equator than toward the pole. Hence, photons from near the equator scatter at a higher rate and so impart a stronger impulse than those from near the pole, thus enhancing the net poleward component of the line-force.

The magnitude of this poleward force is small, generally not much more than 10% of the radial line-force; but the equatorward flow speeds are similarly small, i.e. less than 100 km/s in the WCD model, or only a few percent of the maximum radial speed. Thus, while the radial line-force must be strong enough to overcome the stellar gravity to drive an outflow to terminal speeds of more than 1000 km/s, the poleward latitudinal line-force is unopposed by any other body force, and need only overcome inertial terms characterized by a modest, < 100 km/s equatorward drift. From this perspective, it thus seems clear that the derived nonradial forces should indeed be dynamically quite significant in redirecting the equatorward drift needed for a WCD. The next section presents a scaling analysis that quantifies these arguments.

3.3. STOPPING DISTANCE ANALYSIS FOR WCD INHIBITION

It is instructive to analyze this WCD inhibition effect in simple scaling-law terms. The general idea is to follow up on the above qualitative arguments that even a latitudinal force g_θ that is substantially smaller than than the radial force g_r should be able to stop the relatively slow v_θ associated with wind compression. Let us thus define a "stopping distance" s_o, over which the equatorward flow would be stopped if we suddenly applied the g_θ to a WCD model initially relaxed without nonradial forces. From simple mechanics, this is roughly given by

$$s_o \approx -\frac{v_\theta^2}{2g_\theta}. \tag{6}$$

Comparing this with $s_\theta \equiv r(\pi/2 - \theta)$, the arc distance the material must move to get to the equator ($\theta = \pi/2$), we define a "stopping number",

$$\sigma \equiv s_\theta / s_o = -\frac{2g_\theta r(\pi/2 - \theta)}{v_\theta^2}. \tag{7}$$

For σ order unity or larger, the nonradial forces should substantially alter or inhibit the wind compression. From the WCD models, we typically find an upper limit $v_\theta < V_{rot}/4$. To obtain an estimate for g_θ, we must examime the formulae in Cranmer and Owocki (1995). Ignoring, for simplicity, both

gravity darkening and oblateness, the ratio of the latitudinal component of the line force to the point-star radial force can be written

$$\eta_\theta = \frac{r^2}{R_*^2(\partial v_r/\partial r)^\alpha}\int_\mu^1 d\mu' \int_0^{2\pi} d\phi' \left[\mathbf{n}\cdot\nabla(\mathbf{n}\cdot\mathbf{v})\right]^\alpha \; n_\theta, \tag{8}$$

where $n_\theta = \sqrt{1-\mu'^2}\cos\phi'$, and $\mu_* \equiv \sqrt{1-R_*/r}$. The key is to find a simplification for the projected velocity gradient term, given explicitly by eqn. (41) of Cranmer and Owocki (1995). Following our argument that the main cause of the latitudinal force is the latitudinal gradient of the radial velocity, $\partial v_r/\partial\theta$, let us ignore all terms with v_θ or v_ϕ, keeping only the terms containing v_r. Assuming a characteristic value $\partial v_r/\partial r \approx v/r$, we can then write the projected gradient term as

$$\left[\mathbf{n}\cdot\nabla(\mathbf{n}\cdot\mathbf{v})\right]^\alpha = \left[\frac{\partial v_r}{\partial r} + \frac{\mu' n_\theta}{r}\frac{\partial v_r}{\partial\theta}\right]^\alpha \approx \left(\frac{\partial v_r}{\partial r}\right)^\alpha \left[1+\alpha\mu' n_\theta \frac{\partial v_r/r\partial\theta}{\partial v_r/\partial r}\right], \tag{9}$$

where the latter approximation applies when the latitudinal gradient is small compared to the radial gradient. Applying this in eqn. (9), we find that the integrals can be carried out analytically, with the first term vanishing by the ϕ' integration of n_θ. After some manipulation (e.g. using the definition μ_*), we obtain

$$\frac{g_\theta}{g_r} \approx \eta_\theta \approx \frac{\alpha}{4}\frac{R_*^2}{r^2}\frac{\partial v_r/r\partial\theta}{\partial v_r/\partial r}, \tag{10}$$

where the initial approximation uses the fact that, in the wind region where $\partial v_r/\partial r \approx v/r$, the radial finite-disk correction factor is near unity, and so $\eta_\theta \approx g_\theta/g_r$. Then noting, from the equation of motion, that $g_r \approx v_r(\partial v_r/\partial r)/\alpha$ (i.e., the radial driving force is partitioned roughly in proportion α and $1-\alpha$ between inertia and gravity), we find

$$g_\theta \approx \frac{R_*^2}{4r^2}\;\frac{v_r}{r}\frac{\partial v_r}{\partial\theta} \tag{11}$$

Fig. 2b illustrates that this approximation is in good general agreement with numerical calculations of the line-force.

Finally, we need to parameterize the theta dependence of the radial velocity. For this, let us use the usual "effective escape speed" argument to write

$$v_r(r,\theta) \approx v_o(r)\sqrt{1-\Omega\sin^2\theta}, \tag{12}$$

where $v_o(r) \equiv v_r(r,\theta=0)$ is the polar velocity law. Applying this in eqn. (11), we obtain

$$g_\theta \approx -\frac{R_*^2}{2r^2}\;\frac{v_o^2}{r}\Omega\sin\theta\cos\theta, \tag{13}$$

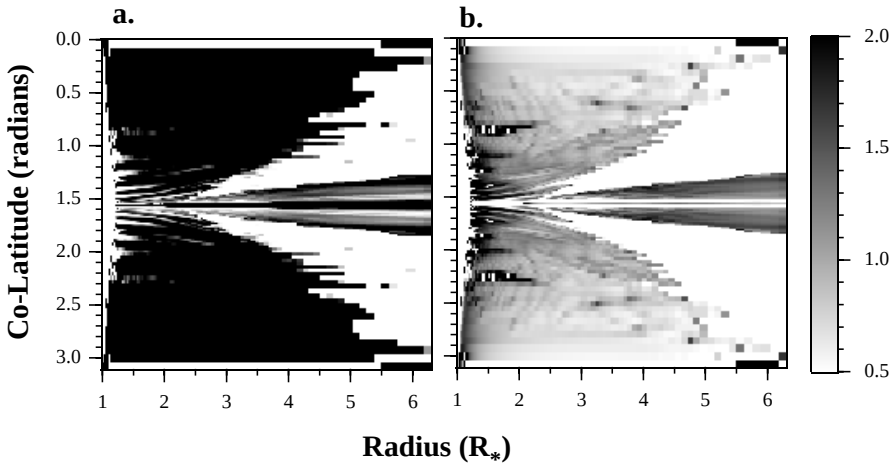

Figure 2. (a.) Grayscale plot of the stopping number, σ, in the S-350 WCD model, scaled over the range $0.5 < \sigma < 2$ for white to black. The dominance of black in almost the entire near-star region shows that the poleward component of the line force is sufficient to significantly alter or reverse the WCD tendency for material to deflect toward the equator. (b.) Grayscale plot of the ratio of the latitudinal force, g , to the terms approximating it on the right-side of eqn. (11), also for the S-350 WCD model, with the same gray scale range as in (a). This shows that this approximation holds within a factor 2 throughout most of the region relevant to WCD inhibition.

which gives for the stopping number,

$$\sigma \approx \frac{v_o^2 R_*^2 \Omega \sin\theta \cos\theta \, (\pi/2 - \theta)}{v_\theta^2 r^2}. \qquad (14)$$

Evaluating this at a characteristic location $r = 2R_*$ and $\theta = \pi/4$, using $v_o(r = 2R_*) \approx v_{o,\infty}/2 \approx v_{esc}/2 = v_{crit}/\sqrt{2}$, and $v_\theta < v_{rot}/4$, we find $\sigma \gtrsim \pi/4$, indicating that this latitudinal force will have a substantial effect in inhibiting the wind compression.

Numerical calculations, e.g. for the S-350 model, confirm these estimates, yielding stopping numbers that range $1 < \sigma < 10$ over the entire wind compression region (fig. 2a). These same models also confirm the accuracy of the scaling estimate in eqn. (11), with surprisingly good agreement ($\lesssim$ factor 2) even in the areas where $\partial v_r / r \partial\theta$ is not necessarily small compared to $\partial v_r / \partial r$ (fig. 2b). The general conclusion is thus that the inibition of WCDs is a quite robust effect, arising almost directly from the tendency of the radial outflow to be slower at lower latitudes.

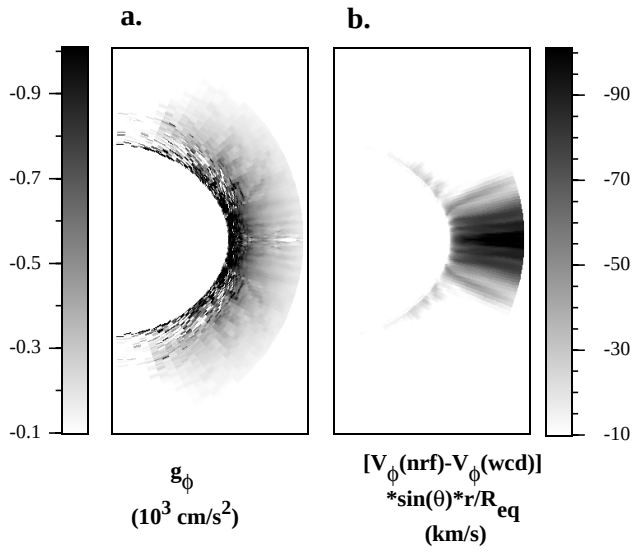

Figure 3. (a.) Grayscale plot of the azimuthal force, g , in the S-350 WCD inibition model of fig. 1b. (b.) Grayscale plot of the azimuthal spindown of wind rotation as a result of the azimuthal line-force. This is given here by the decrease in azimuthal velocity in the WCD inhibition model (fig. 1b) from the initial WCD model (fig. 1a) without nonradial forces, scaled times $(\sin\theta)R \quad /r$, thus making this proportional to the loss of wind angular momentum parallel to the stellar rotation axis.

3.4. SPINDOWN OF WIND ROTATION

Finally, although the 2-D models here have an assumed azimuthal symmetry, there is nonetheless also a nonzero *azimuthal* component of the line-force, which again results from asymmetries in the line-of-sight velocity gradient. Because wind rotation speed declines with increasing radius, the velocity gradient toward the receding stellar hemisphere is greater than that toward the approaching hemisphere. Through eqn. (5), this now implies a net line-force *against* the sense of rotation (Grinin 1978). Its peak magnitude is roughly comparable to that for the poleward line-force, but this is sufficient to cause a modest wind spindown, characterized by about a 25% decrease in the specific angular momentum of the equatorial wind outflow beyond a few tenths of a stellar radius from the surface. Fig. 3a shows grayscale plots of the azimuthal line-force in the S-350 WCD inhibition model (cf. fig. 1b), while fig. 3b shows the resulting azimuthal spindown of the wind in this model. Note that the equatorial regions of the wind have lost more than 100 km/s of their 350 km/s surface rotation speed.

Fig. 4 provides a graphical illustration of the origin of the azimuthal

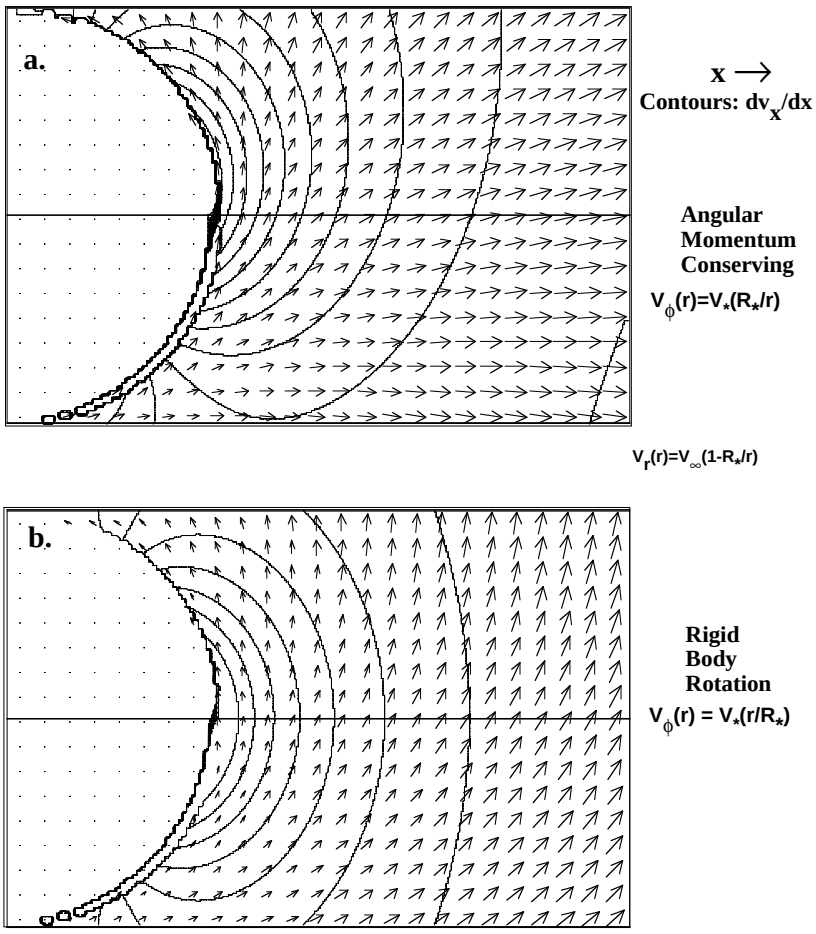

Figure 4. Contours of the projected velocity gradient $\partial v\ /\partial x$ in a direction x (oriented horizontally in the figure), plotted in the equatorial plane of a rotating wind with radial velocity $v\ (r) = v\ \ (1 - R\ /r)$ and azimuthal velocity $v\ (r)$ given either by: (a) angular momentum conservation, $v\ (r) = v\ R\ /r$; or (b) rigid body rotation, $v\ (r) = v\ r/R$. The superposed vectors indicate the sense and magnitude of the total velocity field.

asymmetry in the line resonance that gives rise to a net azimuthal line-force. Consider the flow in the equatorial plane of a simple wind model with a radial velocity given by the ('beta=1') law $v_r(r) = v_\infty(1 - R_*/r)$, and the azimuthal velocity set according to angular momentum conservation, $v_\phi(r) = v_* R_*/r$ (fig. 4a), or to rigid-body rotation, $v_\phi(r) = v_* r/R_*$ (fig.

4b). The contours are of the projected velocity gradient, $\partial v_x/\partial x$, in a given direction x, oriented horizontally on the figure. Because of the azimuthal symmetry of the radiation field, the azimuthal line-force is proportional to the integral,

$$g_\phi \sim \left[\int_{-R}^{R} dy\, y\, \frac{\partial v_x}{\partial x} \right]_r , \tag{15}$$

taken along an arc of constant radius r, over the range $-R_* < y < +R_*$, where y is the vertical coordinate in the figure. The key point is that in fig. 4a, the projected velocity gradient is biased toward the upper part of the plane, indicating the net integral will give a net line-force from radiation originating in the upper, i.e. receding, portion of the stellar surface. By contrast, in the case of rigid rotation shown in fig. 4b, the projected velocity gradient is *symmetric* between the upper and lower half of the plane, and so the azimuthal line-force vanishes in such a rigid rotation wind. Indeed, in the somewhat unlikely case that the azimuthal velocity should have a faster than rigid-body outward increase, the bias would be toward the lower half-plane, leading to a net *spin-up* line-force!

In the other extreme, if the azimuthal velocity falls off faster than for angular momentum conservation, the spin-down force would be stronger. In principle, this raises the possibility of a "runaway wind spindown" solution, in which the azimuthal line-torque leads to a sufficiently steep radial fall-off of azimuthal velocity that the line-torque becomes ever stronger. In practice, we find that overall strength of the line-torque is just a little (i.e. < factor 2) too small to give such runaway solutions, except in rather artificial circumstances, i.e. very low value of α ($\ll 0.5$) or a strong stellar limb brightnening. Though the possibility of a azimuthal line-force was first recognized long ago (Grinin 1978), these latest studies suggest that it can come very close to being a dominant effect. We intend to discuss these analyses further in a future paper.

4. Effect of Gravity Darkening

4.1. UNIFORM WIND DRIVING PARAMETERS

Fig. 1c shows results for the corresponding S-350 model with both nonradial forces and a gravity-darkened surface flux $F(\theta) \sim g_{eff}(\theta)$ (von Zeipel 1924; see also Cranmer & Owocki 1995). In this case, not only is there no disk, but the overall density in the equatorial regions is actually *reduced* relative to that at higher latitudes. This picture is in marked contrast with previous analyses that envisioned an enhanced equatorial mass loss [e.g., eqn. (3); Friend and Abbott 1986], but it agrees well with the predictions of the gravity-darkened mass-flux scaling (4). Despite the reduced gravity near

the equator, the wind mass flux there is now lower, owing to the reduced radiative flux associated with gravity darkening. The superposed vectors further show that the latitudinal velocity is again away from the equator, though with a somewhat lower magnitude than in Figure 1b, owing to the reduced poleward force associated with the reduced radiative flux from the equator.

4.2. EQUATORIAL BI-STABILITY ZONE

The above calculations have assumed fixed values of the CAK parameters (α, k, and δ), but in general these can be expected to vary with variations in, e.g., effective temperature and density. A particularly important example of this is the Lamers and Pauldrach (1991) *Bi-Stability* model for equatorial enhanced winds in B[e] stars. At effective temperatures near 20,000 K, the increased recombination of hydrogen tends to make a wind become optically thick in the Lyman continuum, thus dramatically altering the wind ionization/excitation balance, and so leading to a marked shift of line-driving parameters. The effect can be most easily described in terms of a decreasing CAK exponent α, with a relatively constant line normalization parameter $\bar{Q} \approx 10^3$, related to the usual CAK k constant by $k = \bar{Q}^{1-\alpha}(v_{th}/c)^\alpha/(1-\alpha)$ (Gayley 1995). Within CAK theory, the mass flux varies as $\dot{m} \sim \bar{Q}^{-1+1/\alpha}$, and so adopting this into the scaling formulae in §2, we find for the latitudinal variation of density $\rho \sim \dot{m}/v$,

$$\frac{\rho(\theta)}{\rho_o} = \sqrt{1 - \Omega \sin^2\theta}\,(\Gamma_e \bar{Q})^{1/\alpha - 1/\alpha} \quad , \tag{16}$$

where $\Gamma_e = \kappa_e F/g_{eff}c$ is the surface Eddington factor, which is independent of latitude in the standard von Zeipel (1924) scaling $F \sim g_{eff}$ for gravity darkening. The exponent α is now assumed to vary in latitude, e.g. from a typical O-star value $\alpha_o \approx 2/3$ at the relatively high-temperature pole, to a lower, B-star value $\alpha \approx 1/2$ at lower latitudes, where the rotation brings the effective temperature near or below the critical bi-stability temperature of $\sim$ 20,000 K. The expression here includes the reduced driving from the lower equatorial brightness, an effect that actually was overlooked in the original Lamers and Pauldrach (1991) analysis, cf. their eqn. (4) and our eqns. (3) and (4). For stars with Eddington factors Γ_e not much less than unity, the large intrinsic value of $\bar{Q}$ implies that this shift in α can cause a strong increase in mass flux, as signified by the second term in eqn. (16). For example, for the case $\Gamma_e = 0.5$, $\bar{Q} = 10^3$, $\alpha_o = 2/3$, and $\alpha = 1/2$, this bistability density jump represents a quite large factor, $\sim \sqrt{500} \approx 22$. In principle, this could occur quite abruptly near and below the latitude of the critical temperature, and thus overwhelm the more gradual tendency

for the mass flux to decline with the decreasing radiative flux near the equator. As such, this model remains a viable possibility for explaining moderate increases in equatorial density, such as inferred for B[e] stars.

5. Concluding Remarks

The above results on nonradial forces and gravity darkening are both a surprise, in that they essentially reverse previous theoretical expectations, and a puzzle, in that they apparently contradict observational evidence for enhanced densities in the equatorial regions around rapidly rotating hot-stars. As regards gravity darkening, if convection were to dominate energy transport in the envelope of rapidly rotating stars, then the equatorial darkening could be substantially reduced, or even eliminated (Zhou and Leung 1990). Given the formidable difficulties of multidimensional modelling of convection in rapidly rotating stellar envelopes, this emphasizes the importance of determining reliable observational diagnostics of gravity darkening in such stars (e.g., Howarth and Reid 1993; Reid et al. 1993).

As regards WCD inhibition by nonradial line-forces, we emphasize the following point:

> The WCD inhibition described above is specific to *line-driven* winds, and does *not* imply a failure or weakness of the general WCD paradigm as potentially applied to outflows driven by any other mechanism.

The great success and intuitive appeal of the WCD paradigm stems from the simplicity of its key idea, that material slowly driven radially outward from a star should, by virtue of angular momentum conservation, remain in an orbital plane that intersects the equator. In the context of line-driven flows, however, this key assumption of strictly radial driving represents a serious oversimplification, because of the nonvanishing poleward component of the line-force, which can retard and indeed reverse the equatorward flow essential for a WCD. Moreover, within the standard CAK/Sobolev formalism, this WCD inhibition seems quite robust, arising directly from the tendencies for the line-force to scale with the line-of-sight velocity gradient, and for the wind from a rotating star to be slowest at lower, near-equatorial latitudes. Insofar as winds from O and B stars have traditionally, and quite successfully, been modelled using the CAK, line-driving formalism, this clearly represents a serious challenge for applying the WCD paradigm toward, e.g. Be stars, B[e] stars, and selected O-stars (e.g., HD 93521: Howarth and Reid 1993; Bjorkman et al. 1994) inferred to have enhanced equatorial densities and/or disks. As such, perhaps the findings here can be interpreted as indicating that other mechanisms, e.g. decretion, magnetic loops, or bistability zones, should be examined as ways to produce the disks or equatorial density enhancements inferred in such stars.

However, there are also still questions regarding the applicability of such idealized, CAK line-driven models, particularly for B-star winds. (See, e.g., Cassinelli and Ignace 1997, as well as comments and contributions by J. Cassinelli and J. Bjorkman in these proceedings.) One particularly serious general question (emphasized to us by J. Bjorkman) regards the neglect so far of the strong line-driven flow instabiilty (see, e.g., Owocki 1994 and references therein), which ultimately should break the wind up into multiple dense blobs that might not receive the same poleward driving force. This question needs to be addressed in future work, but it represents a formidable computational challenge to develop tractable methods for evaluating the required *nonlocal* escape integral forms for the line-force (Owocki and Puls 1996) within a multi-dimensional dynamical simulation. Given these remaining questions, it may not yet be appropriate to strictly rule out the WCD model, even for line-driven models of B[e] stars. But though not dead, the line-driven WCD does seem seriously crippled, or at least 'dynamically challenged'.

Whatever the ultimate resolution to these puzzles, we hope that the results here will spur a reexamination and questioning that ultimately leads to a deeper understanding of the nature of hot-star mass loss. It is remarkable that, more than two decades after introduction of the line-driving mechanism in landmark papers by Lucy and Solomon (1970) and CAK, we are still learning fundamentally new aspects of that intricate process.

Acknowledgements

This work was supported in part by NASA grant NAG5-3530. We thank J. Bjorkman, J. Cassinelli, N. Langer, and J. Puls for useful discussions.

References

Abbott, D.C. 1982, ApJ, 259, 282
Bjorkman, J. E., & Cassinelli, J. P. 1993, ApJ, 409, 429
Bjorkman, J. E., Ignace, R., Tripp, T., & Cassinelli, J. P. 1994, ApJ, 435, 416
Castor, J. I., Abbott, D. C., & Klein, R. I. 1975, ApJ, 195, 157 (CAK)
Cassinelli, J. P. & Ignace 1997, in *Luminous Blue Variables: Massive Stars in Transition*, ASP Conf. Series 120, A. Nota & H.J.G.L.M. Lamers, eds., (PASP: San Francisco)
Cranmer, S. R., & Owocki, S.P. 1995, ApJ, 440, 308
Friend, D. B., & Abbott, D. C. 1986, ApJ, 311, 701
Gayley, K. G. 1995, ApJ, 454, 410
Grinin, A. 1978, Sov. Astr., 14, 113
Howarth, I. D. & Reid, A. H. N. 1993, A&A, 279, 148
Ignace, R., Cassinelli, J. P., and Bjorkman, J. E. 1996, ApJ, 459, 671
Kippenhahn, R. & Weigert, A., 1990, *Stellar Structure*, (Springer: Berlin), p. 436
Lamers, H. J. G. L. M., and Pauldrach, A. W. 1991, A&A, 244, L5
Lucy, L. B. & Solomon 1970, ApJ, 159, 879
Owocki, S. P. 1994, Ap. Sp.Sci., 221, 3.

Owocki, S. P., Cranmer, S. R., & Blondin, J. M. 1994, ApJ, 424, 887
Owocki, S. P., Cranmer, S. R., Gayley, K. G. 1996, ApJ, 472, L115.
Owocki, S. P. & Puls, J. 1996, ApJ, 462, 894
Pauldrach, A.W.A., Puls, J. & Kudritzki, R.-P. 1986, A&A, 164, 86
Reid, A. H. N. et al. 1993, ApJ, 417, 320
von Zeipel, H. 1924, MNRAS, 84, 665
Zhou, D. & Leung, K. 1990, ApJ, 355, 271